

## **Interaction of CdTe Nanorods with Bovine Serum Albumin**

*Swades Ranjan Bera<sup>1</sup>, Satyajit Saha<sup>1</sup> and Tapanendu Kamilya<sup>2</sup>*

<sup>1</sup>Department of Physics and Technophysics, Vidyasagar University  
Midnapore-721102, India

<sup>2</sup>Department of Physics, Narajole Raj College, Paschim Medinipur 721211, India  
Email: [swadesbera@gmail.com](mailto:swadesbera@gmail.com)

*Received 1 September 2016; accepted 22 November 2016*

### **ABSTRACT**

In this paper, CdTe nanorods (NRs) have been grown by a simple cost effective chemical reduction route. The grown CdTe NRs are characterized structurally by X-Ray diffraction (XRD) and transmission electron microscopy (TEM). The grown CdTe (NRs) are characterized optically by Optical Absorption, Photoluminescence (PL) study. The XRD pattern confirmed mainly cubic phase of CdTe NRs. We have studied the interaction as well as the formation of bioconjugate of bovine serum albumin (BSA) with CdTe NRs by applying the HRTEM images and the fluorescence quenching approach in combination with the Stern-Volmer and Hill equations. The photoluminescence spectrum shows shallow deep level visible emission due to various defect states. UV-VIS and fluorescence spectra show that a spontaneous binding process occurred between BSA and Cadmium Telluride nanorod. A small red shift of the absorption peak of BSA is observed due to binding of BSA with CdTe NRs. Cadmium Telluride NRs quench the fluorescence emission of BSA. The Stern-Volmer quenching constant, the binding constant and Hill coefficient were also calculated.

**Keywords:** CdTe nanorod; Bovine serum albumin; high resolution transmission electron microscopy; photoluminescence spectra; absorption spectra.

### **1. Introduction**

Nanostructures exhibit many interesting properties different from their bulk properties and it also has a tremendous potential for the industrial applications in many technical fields including photo catalysts, gas sensors, biological detection and imaging, solar cells, photo detectors and UV sensors, nonlinear optical materials, short-wavelength laser diodes, various luminescence devices, etc [1-5]. And due to the quantum confinement, semiconducting nanocrystals show unique extremely interesting optical properties such as sharp and symmetrical emission spectra, photostability and size dependent emission [6-7]. Generally, Gr II-VI, semiconductor nanorods play an important role having application in nano devices. Among the colloidal nanorods (NRs), CdTe (generally Gr-II to Gr-VI) is studied because of the efficiency of its synthesis, the high quality of the resulting sample, and the fact that the optical gap lies in the visible range. Photo luminescent semiconducting nanorods like CdTe NRs have been linked with bio-

recognition molecules such as proteins, peptides etc. and have been used in biological medical fields [7-9] due to their unique properties controlled effects compared with those of the corresponding bulk materials. Photo luminescent NRs have been applied the bio-imaging/labelling [10-11]. The formation of the nanorods-protein conjugates provides the information about conformational changes of protein occurring at the protein-NRs interface. The interaction of nanorods with bio-molecules is studied using various methods such as liquid chromatography, dynamic light scattering, atomic force microscopy, circular dichroism spectroscopy and fluorescence spectroscopy [12-17]. The study of protein-NPs conjugation will provide us with the information of the phenomena occurring at the protein-NPs interface at the molecular level. Whenever NRs come in physiological fluid systems they will interact with the surrounding protein molecules. The protein molecules can strongly bind to NRs and a dynamic layer of proteins is formed on the surface of NRs. This conjugated system is known as "NRs-protein corona" [18-19]. Since the protein corona plays the important roles for the bio-nano interface [20] and will finally determine the destiny of NRs, so it is significant of the evolution process from the discrete protein-NRs conjugates to NR's protein corona [21]. BSA has been one of the most extensively studied proteins, because of its structural homology with human serum albumin.

In this study, CdTe nanorods (NRs) have been grown by chemical reduction route. Sodium borohydride is used to initiate the reaction between CdCl<sub>2</sub> and Tellurium at room temperature. The dispersed samples are characterized structurally and optically. We have been investigated the effect of interaction between bovine serum albumin with CdTe nanorods in aqueous solution using the absorption, fluorescence quenching technique and TEM analysis. We carried out the binding constants and quenching constants.

## **2. Experimental**

### **2.1. Materials**

Bovine Serum Albumin (BSA) was purchased from Sigma-Aldrich Corporation. De-ionized water (resistivity 18.2 MΩ.cm and pH 6.8) used for all experiments was made from a Milli-Q system (Millipore, Bedford, MA). BSA was dissolved in Milli-Q water for a stock solution with a concentration of 0.25 μM. Anhydrous Cadmium Chloride (CdCl<sub>2</sub>), Tellurium Powder (Te), Sodium Borohydride (NaBH<sub>4</sub>), Ethylenediamine (EN, NH<sub>2</sub>CH<sub>2</sub>CH<sub>2</sub>NH<sub>2</sub>) was purchased from Merck, India. All materials were used as starting materials without any purification.

### **2.2. Material preparation**

CdTe NRs were prepared by chemical reduction method as reported elsewhere [23]. Briefly, 603.96 mg of Anhydrous CdCl<sub>2</sub>, 382.8 mg of Tellurium powder and 113.49 mg of sodium borohydride have been taken to prepare different samples at the ratio 1:1:1 at 318K. Ethylenediamine (EDA) has been used as a capping agent. Sodium borohydride has been taken to initiate the reaction at 318K. The magnetic stirring is continued for 3 hours at a constant speed. The as prepared CdTe NRs were dispersed in Millipore water using ultrasonication for 20 mins with the variation in concentration of CdTe NRs from 150 μM to 700 μM. BSA-CdTe NRs mixed solutions were prepared by mixing 0.25 μM BSA with CdTe NRs, ranging from 150 μM to 700 μM with proper ratio.

### 2.3. Characterization

The X-ray diffraction (XRD) pattern on the CdTe NRs samples were recorded by a X-ray diffractometer (miniflex II, desktop-X-ray diffractometer) using Cu- $\alpha$  radiation of wavelength  $\lambda = 1.54 \text{ \AA}$  for  $2\theta$  ranging from  $20^\circ$  to  $70^\circ$ .

For microstructural measurements, the as-prepared CdTe NRs have been dispersed by ultrasonicator. A small drop of dispersed CdTe NRs has been taken on a thin carbon film supported on the copper grid and kept for some time for drying. The Transmission Electron Micro-graph of the as-prepared CdTe NRs samples has been taken using a JEOL-JEM-2010 transmission electron microscope operating at 200 kV. Selected area electron diffraction (SAED) pattern of the said nanorods were also performed.

A small amount of CdTe NRs samples were dispersed for certain minutes by ultrasonicator. Optical absorption measurements of the dispersed samples have been studied in the range of 230 nm–700 nm using a Shimadzu Pharmaspec 1700 UV–VIS Spectrophotometer. Photoluminescence (PL) spectra of the dispersed samples are recorded using Perkin Elmer LS 55 Fluorescence Spectrophotometer equipped with a 1.0 cm quartz cell with a fixed excitation wavelength of 279 nm, and both excitation and emission slits were set up to 5 nm. For the fluorometric titration experiment, 0.8 mL solutions containing different BSA-CdTe NRs ratio numbers with a fixed final BSA concentration of 0.25  $\mu\text{M}$  was prepared.

## 3. Results and discussions

### 3.1. X-ray diffraction (XRD) study

The XRD pattern of the CdTe NRs is shown in figure 1. The unit cell of the crystal was found to be mixture of cubic phase and hexagonal phase with the presence of the peaks C(111), C(200), C(220), H(110), H(112), C(311), C(222), H(022), C(400), C(331) and C(420). The intensities of different diffraction peaks are different, which indicates that the growth of various planes (direction) is different.

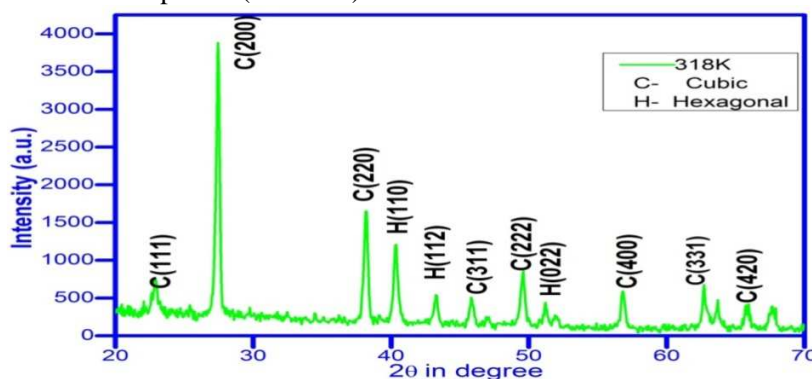


Figure 1. The XRD pattern of the sample CdTe NRs

### 3.2. Morphological studies by TEM

Morphologies of the synthesized samples are shown in fig2. The diameter of the nanorods is in the order of 10nm. Figure 2 (a) shows the nanostructure of pure CdTe with diameter 10 nm. The SAED pattern of pure CdTe nanorods are crystalline nature as shown in figures 2(b). Figures 2(c) and 2(d) show the behavior of the BSA-CdTe nanorods conjugates. HRTEM clearly indicates that core CdTe nanorods is coated by

Swades Ranjan Bera, Satyajit Saha and Tapanendu Kamilya

shell BSA. The SAED pattern of BSA-CdTe NRs is shown in figure 2(d). This images clearly represents that the core CdTe NRs are fully covered with BSA along with shell thickness of ~ 8 nm, matched with dimension of BSA (~8 nm), calculated from protein data bank [22]. The figure 2(e) shows the same conjugate with lower scaling.

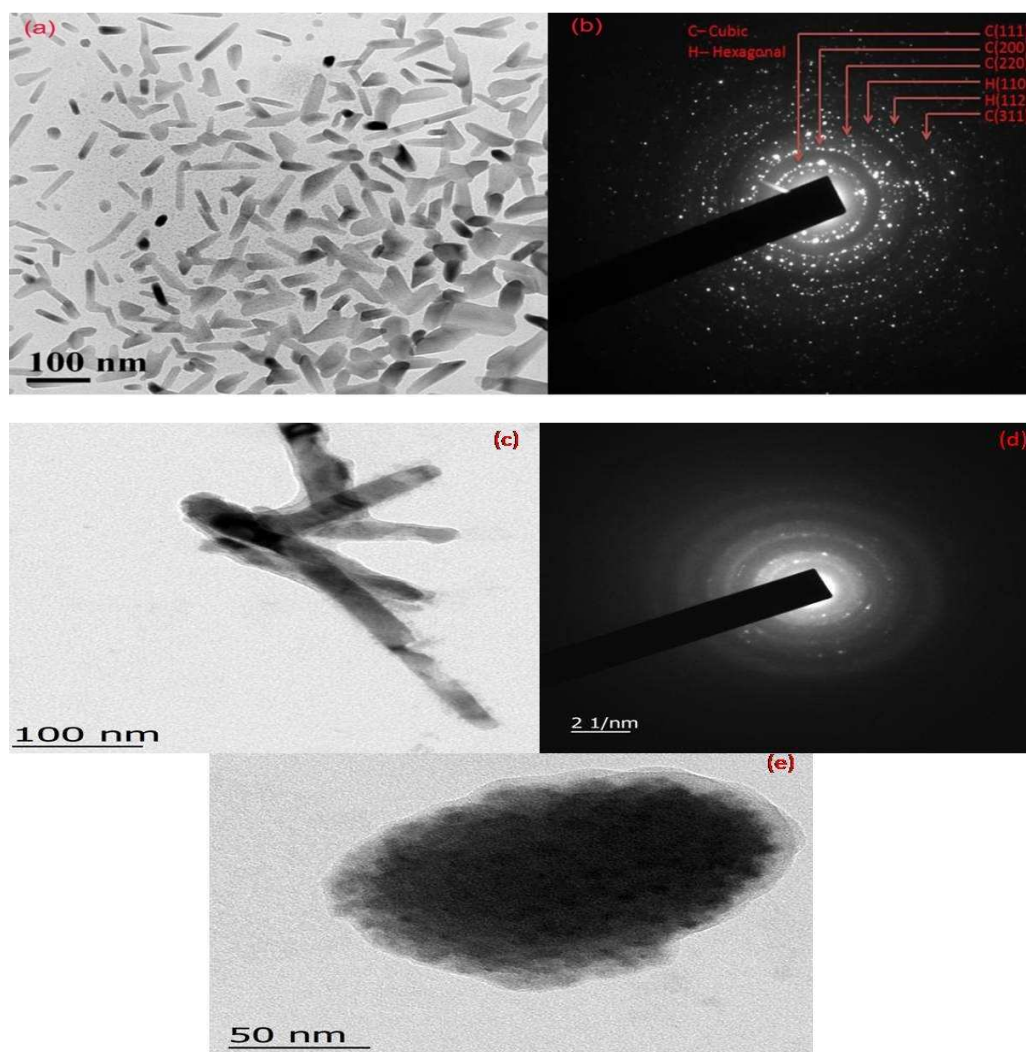


**Figure 2.** HRTEM of (a) pure CdTe NRs; (b) SAED pattern of pure CdTe NRs; (c) CdTe-BSA conjugate; (d) SAED of CdTe-BSA conjugate (e) CdTe-BSA conjugate.

### 3.3 UV-vis spectroscopy study

The figure 3(a) shows the optical absorption spectra of pure CdTe NRs. The figure 1(b) shows the optical absorption spectra of BSA – CdTe NRs. The BSA exhibits absorption peak at 279 nm due to the  $\Pi$ - $\Pi^*$  transition of aromatic amino acid residues [24]. The UV visible spectra presented in Figures 3(b) illustrate the effect of binding of CdTe NRs with bovine serum albumin. In fig. 3(b) our results showed that the BSA absorbance (279 nm)

### Interaction of CdTe Nanorods With Bovine Serum Albumin

increases in increases with  $C_{CdTe}$ . The increase in absorbance intensity of BSA in the presence of CdTe may be due to binding of BSA with CdTe NRs and the formation of the ground state complex [25].

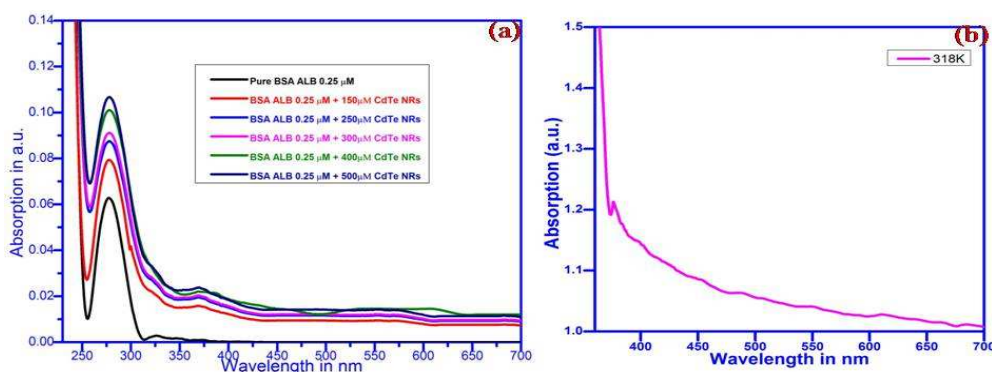


**Figure 3.** Absorption spectra of (a) pure BSA with 0.25  $\mu$ M, and BSA – CdTe NRs complex with 0.25  $\mu$ M of BSA and 150, 250, 300, 400, 500  $\mu$ M of CdTe NRs, (b) Pure CdTe NRs

### 3.4. Fluorescence quenching study

Fluorescence spectroscopy is responsible for the robust BSA-CdTe NRs formation. We employed the fluorescence quenching method [26, 27, 28] to study binding kinetics of the interaction of BSA-CdTe NRs. Figure 4(a) shows the emission spectra of pure CdTe NRs. The photoluminescence spectrum shows shallow deep level visible emission around 575nm due to various defect states. The CdTe NRs-BSA binding kinetics equilibrium has been analyzed by fluorescence quenching measurements. Figure 4(b) shows the emission spectra of pure BSA and BSA-CdTe NRs complex. This figure shows that a quenching of the intensity of the emission of the peaks is more quenched with the increasing addition of CdTe NRs of different concentrations. [28-30].The observed fluorescence quenching probably arises from the energy transfer occurring between BSA and CdTe NRs. The quenching occurs via the adsorption and interaction of the bovine serum albumin residues accessible to the metallic surface of the CdTe NRs. The quenching of fluorescence can be described by the Stern-Volmer equation

$$F_0/F=1+K_{SV} [C]$$

where,  $F_0$  and  $F$  are the fluorescence intensities in the absence and presence of quencher respectively.  $K_{SV}$  is the Stern-Volmer quenching constant.  $[C]$  is the concentration of the quencher. The Stern-Volmer quenching constant which is a measure of the quenching efficiency, has been calculated to  $1.39 \times 10^3 \text{ M}^{-1}$ . The relation between the fluorescence intensity and the quencher concentration is followed by the equation given below [26, 27, 28, 30]

$$\ln \frac{(F_0 - F)}{F} = \ln K_b + n \ln [C]$$

where,  $K_b$  is the binding constant and  $n$  is the Hill coefficient. The Hill equation can be used to analyze the quenching data with more significant parameters. By plotting of  $\ln[(F_0-F)/F]$  vs  $\log[C]$ , the binding constant  $K_b$  and Hill coefficient ( $n$ ) can be calculated from the y-intercept and gradient of the straight line.

The binding constant  $K_b$  and Hill coefficient ( $n$ ) between BSA and CdTe NRs are  $2.74 \times 10^3 \text{ M}^{-1}$  and 0.90 respectively. In addition, we can get the Hill coefficient ( $n$ ) which describes the degree of cooperativity in ligand binding to a surface [31]. If  $n > 1$ , the binding of a ligand is enhanced if there are already other ligands adsorbed to the surface. If  $n < 1$ , the binding of a ligand is weak if there are already other ligands adsorbed to the surface. In cases where  $n = 1$ , the binding of a ligand is independent of other ligands already at the surface. Our results indicate that a negative cooperative take place [24]. According to the result, association energy per particle progressively decreases with further BSA adsorption. The binding of BSA – CdTe NRs conjugates is weak.

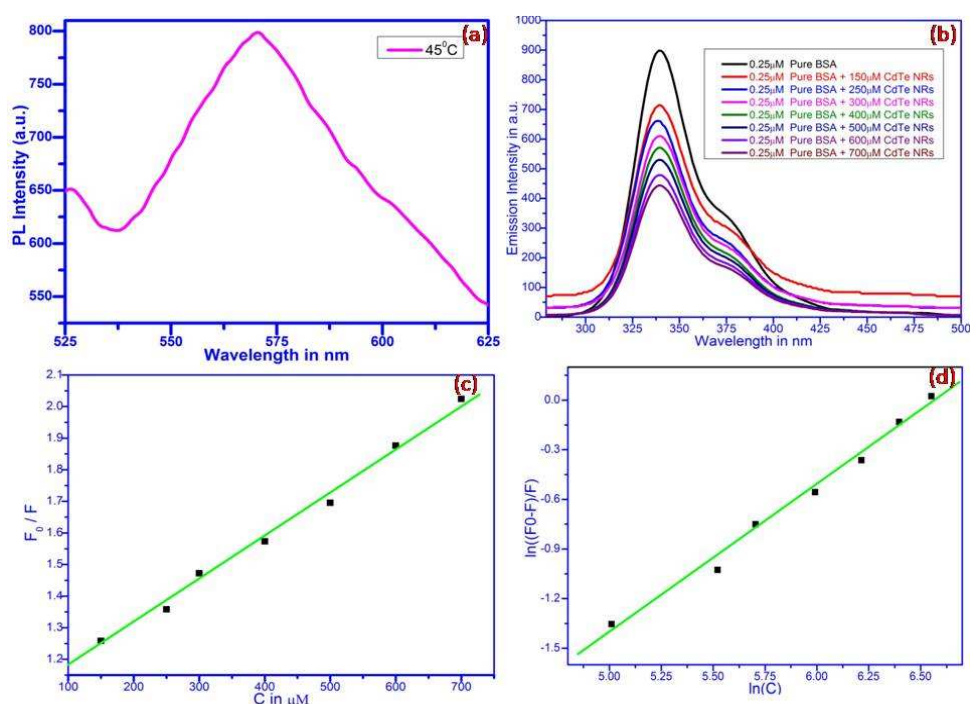


**Figure 4.** Emission spectra of (a) pure CdTe NRs, (b) pure BSA with 0.25  $\mu\text{M}$ , and BSA – CdTe NRs complex with 0.25  $\mu\text{M}$  of BSA and 150, 250, 300, 400, 500, 600, 700  $\mu\text{M}$  of CdTe NRs; (c)  $F_0/F$  vs  $C(\mu\text{M})$ ; (d)  $\ln [(F_0-F)/F]$  vs  $\ln[C]$ .

### 3. Conclusion

We have synthesized and characterized Cadmium telluride nanorods chemically. The average diameter is 10 nm. The interaction of bovine serum albumin- CdTe NRs conjugates is studied through structurally and optically. The emission quenching of the nanorods-BSA system showed a strong interaction phenomenon. The interaction between CdTe nanorods with BSA showed negative cooperative reaction phenomenon. The TEM picture indicates that the NRs are completely covered by BSA molecules. This provides good insight into the interaction of the protein fluorophore BSA with semiconducting CdTe nanorods. This study gives opportunity for potential applications in biotechnology.

### Acknowledgments

Authors are grateful to UGC and DST for their constant financial assistance through SAP and FIST programme to Department of Physics and Technophysics of Vidyasagar University.

### REFERENCES

1. V.P.Singh, J.C.McClure, Design issues in the fabrication of CdS–CdTe solar cells on molybdenum foil substrates. *Sol Energy Mater Sol Cells*, 76 (2003) 369–385
2. X.Duan, C.Niu, V.Sahi, J.Chen, J.W.Parce, S.Empedocles and J.L.Goldman, High-performance thin film transistors using semiconductor nanowires and nanoribbons. *Nature*, 425 (2003) 274–278.
3. S.R.Bera and S.Saha, Fabrication of CdTe/Si heterojunction solar cell, *Applied Nanoscience*, DOI 10.1007/s13204-015-0516-5.
4. P. Capper, *Narrow Gap II-VI Compounds for Optoelectronic and Electromagnetic Applications*, Chapman & Hall, London, UK, 1st edition, 1997.
5. N.Lovergine, P.Prete, L.Tapfer, F.Marzo and M.Mancini., “Hydrogen transport vapour growth and properties of thick CdTe epilayers for RT X-ray detector applications,” *Crystal Research and Technology*, 40(10-11) (2005) 1018–1022.
6. C.Jana, D.Jana, B.Petra, P.Jan, P.Jan and H.Jaromir, Study of Protein Conjugation with Different Types of CdTe Quantum Dots, ICQNM 2013, The Seventh International Conference on Quantum, Nano and Micro Technologies.
7. G.P.C.Drummen, "Quantum Dots-From Synthesis to Applications in Biomedicine and Life Sciences", *Int. J. Mol. Sci.*, 11(1) (2010) 154-163.
8. S.Saha and A.K.Bhunia, Synthesis and Characterization of ZnO Nanoparticles, *Journal of Physical Sciences*, 19 (2014) 109.
9. S.Saha and A.K.Bhunia, Synthesis of Fe<sub>2</sub>O<sub>3</sub> Nanoparticles and Study of its Structural, Optical Properties, *Journal of Physical Sciences*, 17 (2013) 191-195.
10. P.Zrazhevskiy, M.Sena and X.Gao, Designing multifunctional quantum dots for bioimaging, detection, and drug delivery, *Chem. Soc. Rev.*, 39 (2010) 4326-4354.
11. S.Y.Lim, W.Shen and Z.Gao, Carbon quantum dots and their applications, *Chem. Soc. Rev.*, 44 (2015) 362-381.
12. Y.Z.Xie, V.P.Kunets, Z.M.Wang, V.Dorogan, Y.I.Mazur, J.Wu and G.J.Salamo, Multiple stacking of InGaAs/GaAs (731) nanostructures, *Nano- MicroLett.*, 1(1) (2009) 1-3.
13. L.Shao, C.Dong, F.Sang, H.Qian and J.Ren, Studies on Interaction of CdTe Quantum Dots with Bovine Serum Albumin Using Fluorescence Correlation Spectroscopy, *J Fluoresc*, 19(1) (2009) 151-157.
14. B.I.Ipe, A.Shukla, H.Lu, B.Zou, H.Rehage and C.M.Niemeyer, Dynamic Light-Scattering Analysis of the Electrostatic Interaction of Hexahistidine-Tagged Cytochrome P450 Enzyme with Semiconductor Quantum Dots, *Chemphyschem*, 7(5) (2006) 1112-1118.
15. T.Pons, H.T.Uyeda, I.L.Medintz and H.Mattoussi, Hydrodynamic Dimensions, Electrophoretic Mobility, and Stability of Hydrophilic Quantum Dots, *J. Phys Chem B*, 110(41) (2006) 20308-20316.
16. B.J.Nehilla, T.O.Vu and T.A.Desai, Stoichiometry-Dependent Formation of Quantum Dot–Antibody Bioconjugates: A Complementary Atomic Force

- Microscopy and Agarose Gel Electrophoresis Study, *J Phys Chem B*, 109(44) (2005) 20724-20730.
17. V.Poderys, M.Matulionyte, A.Selskis and R.Rotomskis, Interaction of Water-Soluble CdTe Quantum Dots with Bovine Serum Albumin, *Nanoscale Res Lett.*, 6 (2011) 9.
  18. T.K.Das, A.K.Bhunia, T.Kamilya and S.Saha, Optical and Structural analysis on the interaction of ZnSe Nanorods with L-Tryptophan, *Journal of Chemical and Pharmaceutical Research*, 8 (2016) 702-707.
  19. B.A.Korgel, D.Fitzmaurice, Self-Assembly of Silver Nanocrystals into Two-Dimensional Nanowire Arrays, *Adv. Matter*, 10 (1998) 661.
  20. M.Lundqvist, J.Stigler, G.Elia, I.Lynch, T.Cedervall and K.A.Dawson, The Evolution of the Protein Corona around Nanoparticles: A Test Study, *Proc. Natl. Acad. Sci. U. S. A.*, 105 (2008) 14265-14270.
  21. J.Guo, R.Zhong, W.Li, Y.Liu, Z.Bai, J.Yin, J.Liu, P.Gong, X.Zhao and F.Zhang., Interaction Study on Bovine Serum Albumin Physically Binding to Silver Nanoparticles: Evolution from Discrete Conjugates to Protein Coronas, *Applied Surface Science*, DOI: <http://dx.doi.org/doi:10.1016/j.apsusc.2015.09.247>.
  22. Protein Data Bank
  23. S.Saha, S.R.Bera, Growth and Characterization of CdTe Nanostructures Grown by Chemical Reduction Route, *International Journal of Metallurgical & Materials Science and Engineering (IJMMSE)*, 3(1) (2013) 37-40.
  24. S.Saha, T.Kamilya, R.Bhattacharya and A.K.Bhunia, Unfolding of Blood Plasma Albumin Protein in Interaction with CdS Nanoparticles, *Sci. Adv. Mater.*, doi:10.1166/sam.2014.1680.
  25. A.K.Bhunia, P.K.Samanta, S.Saha and T.Kamilya, ZnO nanoparticle-protein interaction: Corona formation with associated unfolding, *Appl. Phys. Lett.*, 103 (2013) 143701.
  26. R.Zhong, Y.Liu, P.Zhang, J.Liu, G.Zhao and F.Zhang, Discrete Nanoparticle-BSA Conjugates Manipulated by Hydrophobic Interaction, *Acs Appl. Mater. Interfaces*, 6 (2014) 19465-19470.
  27. M.Yuan, R.Zhong, X.Yun, J.Hou, Q.Du, G.Zhao and F.Zhang, A fluorimetric study on the interaction between a Trp-containing beta-strand peptide and amphiphilic polymer-coated gold nanoparticles, *Luminescence*, (2015) DOI 10.1002/bio.2920.
  28. Y.S.Liu, P.Zhang, R.B.Zhong, Z.J.Bai, J.Guo, G.F.Zhao and F.Zhang, Fluorimetric study on the interaction between fluoresceinamine and bovine serum albumin, *Nucl. Sci. Tech.*, 26 (2015) 030505.
  29. J.R.Lakowicz, Principles of fluorescence spectroscopy, 3<sup>rd</sup> Edition, Springer Science & Business Media, 2007.
  30. S.P.Boulos, T.A.Davis, J.A.Yang, S.E.Lohse, A.M.Alkilany, L.A.Holland and C.J. Murphy, Nanoparticle-Protein Interactions: A Thermodynamic and Kinetic Study of the Adsorption of Bovine Serum Albumin to Gold Nanoparticle Surfaces, *Langmuir*, 29 (2013) 14984-14996.
  31. J. N.Weiss, The Hill equation revisited: uses and misuses, *FASEB J.*, 11 (1997) 835-841.